

# The Dipole Moment (DM) and Recursive Update in Frequency Domain (RUFD) Methods: Two Novel Techniques in Computational Electromagnetics



Raj Mittra  
Chiara Pelletti  
Kadappan Panyappan  
Agostino Monorchio

## 1. Introduction

In this paper, we begin by introducing a novel concept for formulating electromagnetic simulation problems that is based on the use of the Dipole Moment (DM) approach, which has several desirable features. First, it circumvents the need to deal with the singularity that is inherently encountered during the process of evaluating the matrix elements in the conventional Method of Moments (MoM) formulation based on the Green's function approach. Second, it handles both dielectric and conducting materials, be they lossy or lossless, in a universal manner, without employing different starting points for the formulation. This enables us to handle inhomogeneous problems in a convenient manner using a single formulation. Third, it does not suffer from the so-called "low-frequency breakdown" problem in the conventional MoM formulation, which is presently handled by using special basis functions, such as the loop-star. Fourth, it enables us to hybridize with finite methods to solve multi-scale problems in a convenient manner.

As is well known, with the advent of sub-micron technologies and increasing awareness of electromagnetic interference and compatibility (EMI/EMC) issues, designers are often interested in deriving full-wave solutions of complete systems. These take into account a wide variety of complex environments in which an antenna or a scatterer may be located. However, deriving full-wave solutions of such complex problems is challenging, especially when dealing with those that involve multi-scale geometries with very fine features. The well-established methods, such as the time-domain technique, FDTD, as well as the frequency-domain methods, FEM and MoM, are often pushed to the

limits of their capabilities when attempting to simulate these types of problems. Our objective in this work is to present a new physics-based formulation, namely the Dipole Moment approach, which is well suited for addressing the above-mentioned problems.

Since the Dipole Moment formulation does not employ the Green's functions, or the vector and scalar potentials, it helps to circumvent two of the key sources of difficulties in the conventional MoM formulation. These are the singularity and low-frequency problems. Specifically, we show that there are no singularities that we need to be concerned with in the Dipole Moment formulation. This therefore obviates the need for special techniques designed to deal with the integration of these singularities. Yet another salutary feature of the Dipole Moment approach is its ability to handle thin and lossy structures, regardless of whether they are metallic or dielectric types, or even combinations thereof. The Dipole Moment formulation can handle these types of objects with ease, without running into ill-conditioning problems. This is true even for very thin wire-like or surface-type structures, which lead to poorly-conditioned MoM matrices, when these problems are formulated in the conventional manner using the Green's function. The technique is valid over the entire frequency range, from low to high, and, as mentioned before, it does not require us to switch to special basis functions to mitigate the so-called "low frequency" problem.

We should point out that the underlying concept of the Dipole Moment approach is similar to the well-known Discrete Dipole Approximation (DDA) [1], which is often used in physics. The Discrete Dipole Approximation defines a lattice described by the locations and distances

---

*Raj Mittra, Chiara Pelletti, and Kadappan Panyappan are with the EMC Lab, 319 Electrical Engineering East, Penn State University, University Park, PA 16802; e-mail: mittra@engr.psu.edu. Chiara Pelletti and Agostino Monorchio are with the Department of Information Engineering, University of Pisa, Via Caruso, I-56126 Pisa, Italy.*

*This is an invited Review of Radio Science from Commission B*

between an array of elements, and then builds and solves a matrix equation by accounting for the contributions on each element due to all of the others, as well as due to the incident field. Despite this similarity, there are two main differences between the Dipole Moment and Discrete Dipole Approximation approaches. First, in contrast to the Discrete Dipole Approximation, the Dipole Moment approach utilizes a spherical building block, for which the associated scattered fields are available in closed forms. Second, the Discrete Dipole Approximation solves a matrix equation for the weights of the polarizations, while the Dipole Moment solves for the weights of the dipole moments, instead.

One consequence of these differences in the two formulations is that unlike the Discrete Dipole Approximation, the Dipole Moment approach can handle arbitrary dielectric and/or PEC objects, or combinations thereof.

The paper also introduces a complementary CEM (computational electromagnetics) algorithm, namely RUF (Recursive Update in Frequency Domain). This is a general-purpose frequency-domain technique, which still preserves the salutary features of the time-domain methods. Unlike other frequency-domain Maxwell solvers, Recursive Update in Frequency Domain neither relies upon iterative nor on inversion techniques. The algorithm also preserves the advantages of the parallelizability, which is a highly desirable attribute of computational electromagnetics solvers using the difference form of Maxwell's equations. Since Recursive Update in Frequency Domain solves Maxwell's equations in a recursive manner without using either iteration or inversion, the problems of dealing with ill-conditioned matrices or constructing robust pre-conditioners are totally avoided. Also, as a frequency-domain solver, it can conveniently handle dispersive media, including plasmonics, although special treatments are needed when  $\epsilon$  and/or  $\mu$  are negative.

It is well known that the conventional time-domain technique, namely the FDTD, demands extensive computational resources when solving either low-frequency problems or when dealing with dispersive media. Not only the MoM, but even FEM-based techniques, also suffer from the low-frequency problem. It is thus evident that a technique that can deal with the low-frequency problem without using pre-conditioners and/or special basis functions would be a very desirable addition to the computational electromagnetics repertoire. An enhanced version of the Recursive Update in Frequency Domain, namely vCFDTD, is also mentioned, and is designed to fill this gap in a seamless and numerically efficient manner.

Finally, the paper shows how the two methods can be blended to yield a hybrid approach, referred to herein as Dipole Moment–Recursive Update in Frequency Domain, to handle multi-scale problems in a convenient manner.

## 2. Dipole Moment Approach

### 2.1 Introduction to Dipole Moment Method

Formulating integral equations via the use of Green's function is a well-established and universally accepted method [2-4], which has been a staple for computational electromagnetics problems for many years. However, as alluded to earlier, MoM requires special treatment at low frequencies, and needs to deal with the singular and/or hyper-singular behaviors of the Green's function. Additionally, both frequency-domain techniques, FEM and MoM, experience difficulties when handling multi-scale geometries because the associated matrices for these problems can be ill-conditioned. In this section, we introduce a universal MoM-like, Dipole-Moment-based formulation [5] to obviate the disadvantages of the conventional frequency-domain techniques.

### 2.2 Dipole Moment Concept

To develop the Dipole Moment concept, we first consider our building block, a sphere, which is illuminated by a plane wave. The resulting scattered fields can be determined analytically because of its spherical symmetry. A PEC sphere of radius  $a$ , immersed in free space and illuminated by a plane wave  $E_x = E_0 e^{-jkz}$ , produces the following scattered electric far fields in the limit of  $ka \rightarrow 0$ :

$$\lim_{ka \rightarrow 0} E_{\theta}^s = E_0 \frac{e^{-jkr}}{kr} (ka)^3 \cos \phi (\cos \theta - 1/2), \quad (1a)$$

$$\lim_{ka \rightarrow 0} E_{\phi}^s = E_0 \frac{e^{-jkr}}{kr} (ka)^3 \cos \phi (1/2 \cos \theta - 1). \quad (1b)$$

The above Equation (1) is derived by using spherical wave functions [6]. Upon closer analysis, we can recognize the fact that Equation (1) resembles the far fields radiated from an  $x$ -directed electric dipole and a  $y$ -directed magnetic dipole, with moments given by

$$Il_x = E_0 \frac{j4\pi}{\eta k^2} (ka)^3, \quad (2a)$$

$$KI_y = E_0 \frac{2\pi}{jk^2} (ka)^3. \quad (2b)$$

Along the same lines, the equivalent dipole moments for a lossless dielectric sphere of radius  $a$ , with a relative dielectric constant of  $\epsilon_r$  and a relative permeability of  $\mu_r$  are found to be

$$Il_x = E_0 \frac{j4\pi}{\eta k^2} (ka)^3 \frac{\epsilon_r - 1}{\epsilon_r + 2}, \quad (3a)$$

$$Kl_x = E_0 \frac{2\pi}{jk^2} (ka)^3 \frac{\mu_r - 1}{\mu_r + 2}. \quad (3b)$$

Equation (3) can be readily modified for a lossy medium by replacing the real valued  $\epsilon_r$  and  $\mu_r$  with their complex permittivity,  $\epsilon$ , and permeability,  $\mu$ , respectively. It is important to note the fact that the magnetic dipole moment goes to zero for non-magnetic media with  $\mu_r = 1$ , and similarly, the electric dipole moment goes to zero for magnetic media with  $\epsilon_r = 1$ .

The dipole-moment representation of a scatterer therefore generates the same *far* fields as those scattered by the original objects.

However, what has not been realized in the past, and what can be proven analytically [7], is that for a sphere with a radius that is electrically small, the dipole-moment fields exactly match the original fields scattered by the sphere, all the way up to its surface.

## 2.3 Dipole Moment Formulation

### 2.3.1 Formulation for PEC Objects

When formulating a problem that involves only PEC objects, the first step is to represent the original scatterer

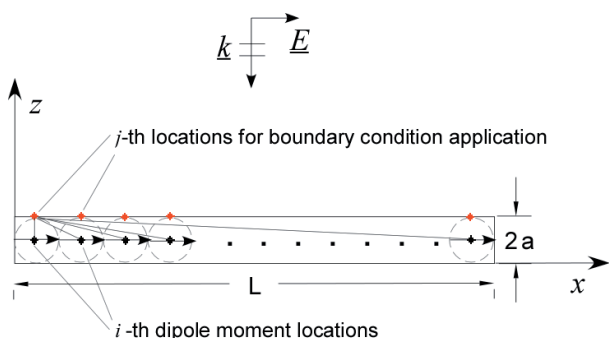


Figure 1a. A PEC wire of length  $L$  and thickness  $2a$ , discretized with equivalent Dipole Moments.

by using a collection of PEC spheres. Next, these spheres are replaced by their corresponding dipole moments (DMs) (see Figure 1a). We can also aggregate a set of the dipole moments, used to form a suitable set of macro-basis functions, as shown in Figure 1b.

The macro-basis-function (MBF) concept is illustrated in Figure 1b for the representative example of a PEC wire, where a set of dipole moments is grouped under the envelope function,  $I(z)$ . The fields produced by a macro-basis function are expressed as a superposition of the fields radiated by the dipole moments located below the envelope, the weights of which correspond to the value of the envelope function at its location. It is possible to show that when  $\Delta z$  approaches zero, the summation of the fields radiated by the dipole moments weighted by the envelope function converges to a closed-form expression for the fields, which is identical to that radiated by a wire with sinusoidal current distribution [8]. The parallel and perpendicular components of the electric fields radiated by the macro-basis function are expressed as

$$E_{\parallel} = -j30 \left[ \frac{e^{-j\beta R_1}}{R_1} + \frac{e^{-j\beta R_2}}{R_2} - 2 \cos(\beta H) \frac{e^{-j\beta r}}{r} \right] \quad (4a)$$

$$E_{\perp} = \frac{j30}{\rho} \left[ (z-H) \frac{e^{-j\beta R_1}}{R_1} + (z+H) \frac{e^{-j\beta R_2}}{R_2} - 2z \cos(\beta H) \frac{e^{-j\beta r}}{r} \right] \quad (4b)$$

where  $R_1$ ,  $R_2$ , and  $r$  represent the distances between the top, bottom, and center of the wire and observation point,  $P$ .  $\rho$  is the radial distance between the center of the wire and the observation point in a cylindrical coordinate system.

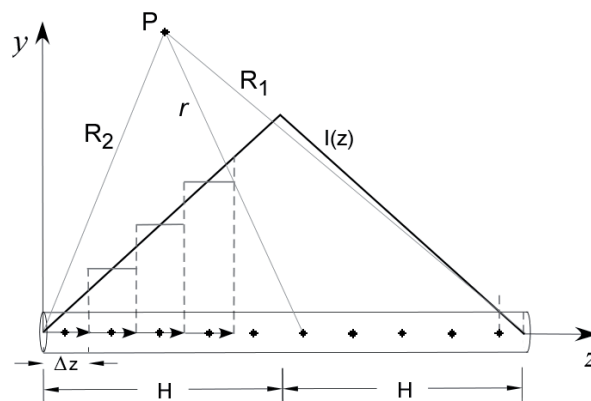


Figure 1b. A representative scheme for the computation of the fields radiated by a macro-basis function.

The concept of triangular macro-basis functions, designed for wires, has also been extended to rooftop types of basis functions that are suitable for discretizing planar or curved surfaces [9]. The fields radiated by the spheres (dipole moments) lying underneath the rooftop can again be expressed in closed form.

We next evaluate the electric fields generated by these macro-basis functions, and compute the reactions between them. We use the same testing functions as the basis functions (Galerkin's method) to generate the elements of the MoM matrix. The right-hand side of this matrix is obtained by applying the boundary condition

$$E_{inc}^{tan} + E_{scat}^{tan} = 0 \quad (5)$$

on the total tangential  $E$  field by testing it with the same functions as those used to generate the matrix elements. For an incident  $E$  field polarized along  $z$ , the matrix equation for a thin PEC rod oriented along  $z$ , modeled by using  $N$  macro-basis functions, has the form

$$\begin{bmatrix} E_z^{11} & E_z^{12} & E_z^{13} & \dots & E_z^{1N} \\ E_z^{21} & E_z^{22} & E_z^{23} & \dots & E_z^{2N} \\ \vdots & \vdots & \vdots & \vdots & \vdots \\ E_z^{N1} & E_z^{N2} & E_z^{N3} & \dots & E_z^{NN} \end{bmatrix} \times \begin{bmatrix} I_z^1 \\ I_z^2 \\ \vdots \\ I_z^N \end{bmatrix} = \begin{bmatrix} E_{z-inc}^1 \\ E_{z-inc}^2 \\ \vdots \\ E_{z-inc}^N \end{bmatrix}, \quad (6)$$

where  $I_z^n$  represents the effective dipole moment of the  $n$ th macro-basis function directed along  $z$ ,  $E_{z-inc}^n$  represents the tangential incident field component at the location of the  $n$ th macro-basis function, and  $E_z^{mn}$  represents the scattered field component along  $z$  on the  $m$ th macro-basis function by the  $n$ th macro-basis function.

The matrix Equation (6) is solved for the  $I$  s, the coefficient of the macro-basis functions, to construct the desired solution for the induced current.

### 2.3.2 Formulation for Dielectric Objects

The first step in the formulation of the dielectric scattering problem essentially follows the case of PEC objects, in that we again represent the original scatterer as a collection of small-size dielectric spheres. As before, we go on to replace these spheres with their corresponding dipole moments, and use them to form a set of macro-basis functions. At this point, we differ from the PEC case and generate the MoM matrix by imposing a boundary condition, but apply a consistency condition, Equation (7), on the tangential  $E$  field, which reads

$$\varepsilon_0 (\varepsilon_r - 1) (\underline{E}_{inc} + \underline{E}_{scat}) = F (I\underline{I}). \quad (7)$$

The consistency factor,  $F$ , can be derived by considering a single sphere located at  $(x_0, y_0, z_0)$ , and matching the polarization currents through Equation (7), where  $\underline{E}_{inc}$  represents the incident electric field at  $(x_0, y_0, z_0)$ , and the electric dipole moment is defined in Equation (3a).

On the surface of the sphere, the fields radiated by the electric dipole moment are given by

$$E^s = -\frac{I\underline{I}}{4\pi} e^{-jka} \left( \frac{j\omega\mu}{a} + \frac{\eta}{a^2} + \frac{1}{j\omega\varepsilon a^3} \right) \sin \frac{\pi}{2} \quad (8a)$$

As  $ka \rightarrow 0$ , Equation (8a) reduces to

$$E^s \approx -\frac{I\underline{I}}{4\pi} \left( \frac{1}{j\omega\varepsilon a^3} \right). \quad (8b)$$

We next substitute Equation (8b) and use the expression for  $I\underline{I}$  from Equation (3a) in Equation (7). Simplifying the resulting expression, we obtain

$$F = -\frac{3j}{4\pi\omega a^3}. \quad (9)$$

In the above representation, we have matched the polarization currents, because the quantities we are dealing with are volume distributed. It is important to note that the scattered field is calculated at the surface of the sphere and is assumed to be the same as it is at the center, since the sphere is small.

## 2.4 Numerical Results

### 2.4.1 PEC Objects

For the first example, we considered a PEC sphere with a diameter of  $\lambda_0/60$  at 10 GHz. It was illuminated by a plane wave, incident from  $x$  and polarized along  $z$ , as shown in Figure 2a. Figure 2b compares the scattered  $E_z$  fields at  $x = \lambda_0/46$ , calculated by using the Dipole Moment approach as described in Section 2.3.1, with those obtained from Mie series [6], for different frequencies. The comparison, which was seen to be good, served to demonstrate that the Dipole Moment approach yields the scattered fields accurately not just in the far field – as is normally stated in textbooks – but all the way up to the surface of the scatterer.

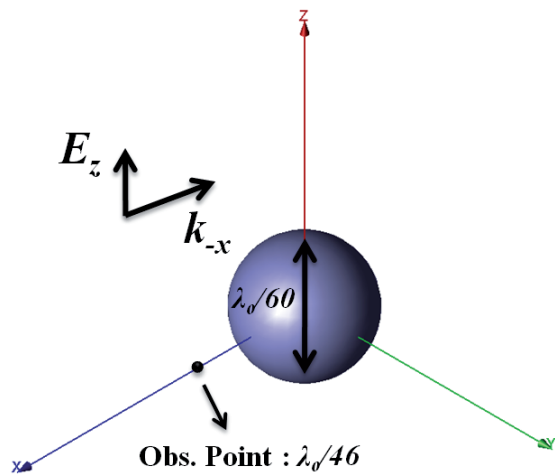


Figure 2a. A PEC sphere.

## 2.4.2 Dielectric Scatterers

To illustrate the universal nature of the Dipole Moment formulation, we next considered a square-shaped dielectric plate with  $\epsilon_r = 6$ , which was  $\lambda_0/40$  on the side, and with a thickness of  $\lambda_0/400$ . The plate was illuminated by a plane wave traveling along the negative  $z$  direction, as shown in Figure 3a. The backscattered field, calculated by using the Dipole Moment approach described in Section 2.3.2, is presented in Figure 3b, which also compares these results with the corresponding results from a commercial MoM package. It should be pointed out that experience shows that when the conducting material in the thin plate is replaced by a dielectric, which may in general be lossy, many of the computational electromagnetics codes – both MoM and finite types – have difficulty in handling the problem. However, the Dipole Moment approach has no difficulty in solving this problem, and it does not employ approximations such as the impedance boundary condition, which may not be accurate for the problem at hand.

## 2.5 Performance Enhancement

The method described in Section 2.3, although it is accurate and captures all the physics, is not the most efficient from a numerical point of view. This is because the number of spheres used to represent a three-dimensional object can grow very rapidly if the diameter of the sphere is small, as is often the case for thin rods and sheets. For instance, for a thin-wire scatterer, the diameters of the spheres used to represent it are the same as that of the wire. Hence, for the example shown in Figure 2, the number of constituent spheres needed to form the plate can be quite large, even when the length of the plate is relatively small. However, as pointed out earlier, the number of unknowns can be significantly reduced and made comparable to that used in the conventional MoM formulation via the use of macro-basis functions. We can also further improve the computational

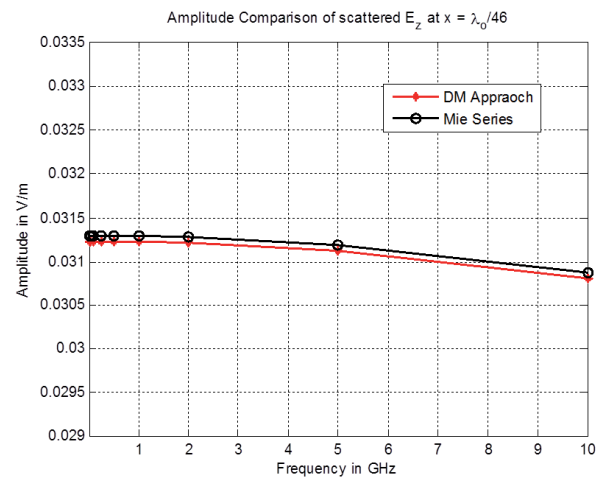


Figure 2b. A comparison of the amplitudes of the backscattered  $E$  fields using the Dipole Moment and Mie series approaches.

efficiency of the method by using techniques such as the Characteristic Basis Function Method (CBFM) [10], the Fast Matrix Generation algorithm [11], or combinations thereof.

## 2.6 Observations

In this section, we have presented a novel physics-based approach for formulating MoM problems, which is based on the use of dipole moments (DMs), as opposed to the conventional Green's functions. The absence of the Green's function, as well as the vector and scalar potentials, helps to eliminate two of the key sources of difficulties in the conventional MoM formulation, namely the singularity and low-frequency problems. Specifically, we have argued that there are no singularities that we need to be concerned with in the Dipole Moment formulation. Hence, this obviates the need for special techniques for integrating these singularities.

Yet another salutary feature of the Dipole Moment approach is its ability to handle thin and lossy structures, whether they be metallic, dielectric-type, or even combinations thereof. We have found that the Dipole Moment formulation can handle these types of objects with ease, without running into ill-conditioning problems. This is true even for very thin wire-like or surface-type structures, which lead to ill-conditioned MoM matrices when these problems are formulated in the conventional manner.

The technique is valid over the entire frequency range, from low to high, and it does not require the use of loop-star types of basis functions in order to mitigate the low-frequency problem. The Dipole Moment formulation is universal, can be used for both PEC and dielectric objects, and requires only a relatively minor change in the formulation when we go from PEC to dielectric scatterers. The approach is also well suited for hybridization with finite methods, such as the FEM and the FDTD. Such an embellishment renders it suitable for conveniently and efficiently handling multi-scale problems.

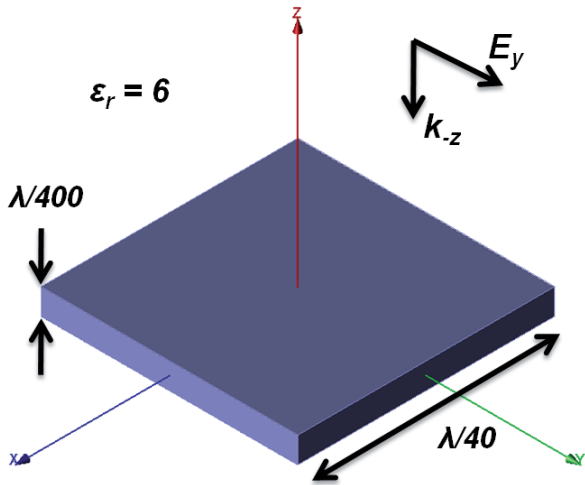


Figure 3a. The simulated dielectric plate.

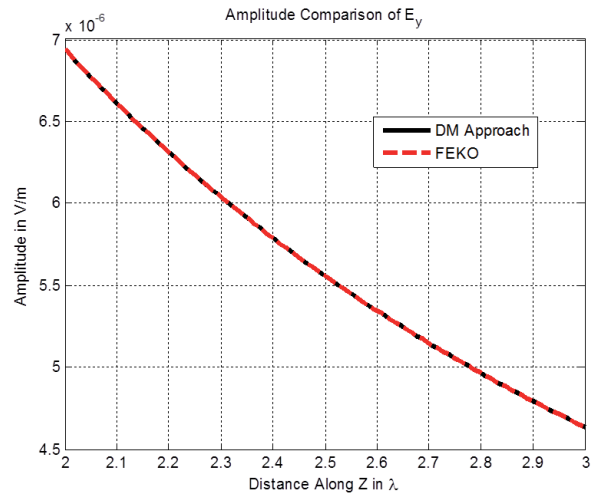


Figure 3b. A comparison of the amplitudes of the back-scattered  $E$  fields for Dipole Moment and FEKO.

### 3. Recursive Update in Frequency Domain

#### 3.1 Introduction

The FDTD time-domain technique is a versatile algorithm, and handles Cartesian geometries with great ease. It has also been generalized to deal with arbitrarily shaped objects by using the conformal FDTD algorithm. However, as is well known, the FDTD algorithm requires long running times when an accurate solution is desired at low frequencies. The method is also not best suited for dealing with dispersive media, unless a convenient model for the same can be found to make it tractable in the time domain. Furthermore, the convergence of the FDTD is slow when analyzing high- $Q$  structures, since the time signature lingers on for a very long period and, hence, requires us to use a large number of time steps to derive an accurate solution. In this section, we first introduce a novel method, called RUF (Recursive Algorithm Frequency Domain). This is a general-purpose frequency-domain technique, which still preserves the salutary features of the time-domain methods, but which neither relies upon iterative schemes nor on inversion techniques. The algorithm also preserves the advantages of parallelizability, which is a highly desirable attribute of computational electromagnetics solvers such as the FDTD. The basic concept of the Recursive Update in Frequency Domain method – which was first introduced by Pflaum et al. in a recent publication [12] – is modified herein to render it considerably more numerically efficient than the original approach.

#### 3.2 Recursive Update in Frequency Domain Algorithm

In common with the FDTD, the Recursive Update in Frequency Domain algorithm begins by using the difference

form of Maxwell's equations to discretize the equations. It next utilizes a leap-frog algorithm, also similar to the FDTD, as proposed by Yee [13]. Consequently, Recursive Update in Frequency Domain may be viewed as the frequency-domain counterpart of the FDTD. This is because it solves the computational electromagnetics problem by using a recursive updating procedure, rather than via a matrix solution (based on inversion or iteration) as commonly employed by other frequency-domain methods. As a frequency-domain solver, Recursive Update in Frequency Domain handles dispersive media with relative ease, although it does require special treatment if the material properties ( $\epsilon$  and/or  $\mu$ ) are negative. The formulation is based on modifying the original Maxwell's equations into a form that is convenient for recursive updating. These modified equations, originally introduced in [12], are given by

$$\frac{e^{j\omega\tau} \hat{E}_h^{n+1} - \hat{E}_h^n}{\tau} = \frac{1}{\epsilon} \nabla_h \times \hat{H}_h^{n+1/2} e^{j\omega\tau/2} - \frac{\sigma}{\epsilon} \hat{E}_h^{n+1} e^{j\omega\tau} + S_E, \quad (10a)$$

$$\frac{e^{j\omega\tau/2} \hat{H}_h^{n+1/2} - e^{-j\omega\tau/2} \hat{H}_h^{n-1/2}}{\tau}$$

$$= \frac{1}{\mu} \nabla_h \times \hat{E}_h^n - \frac{\sigma^*}{\mu} \hat{H}_h^{n+1/2} e^{j\omega\tau/2} + S_H, \quad (10b)$$

where  $\tau$  denotes the discrete iteration step,  $h$  is the mesh size,  $\hat{E}_h^n$  is the complex weight of the approximated electric-field vector at the point  $n\tau$ ,  $\hat{H}_h^{n+1/2}$  is the

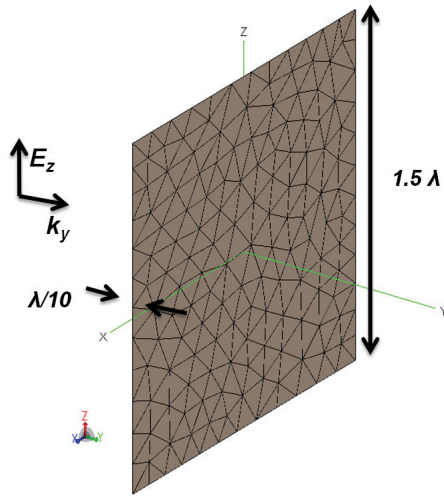


Figure 4a. The simulated PEC slab.

corresponding weight of the magnetic-field vector at the point  $(n+1/2)\tau$ , and  $S_H$  and  $S_E$  are the discrete source terms associated with the excitation.

If we let  $\tau$  tend to zero in Equation (10), assume that  $\hat{E}_h^{n+1} \approx \hat{E}_h^n$  and that  $\hat{H}_h^{n+1/2} \approx \hat{H}_h^{n-1/2}$  in the limit, and use the fact that

$$\lim_{\tau \rightarrow 0} \frac{e^{j\omega\tau} - 1}{\tau} = j\omega, \quad (11)$$

we can show that

$$\hat{E}_{h,\tau=0} = \lim_{\tau \rightarrow 0} \hat{E}_h^n(\tau) \quad \text{and} \quad \hat{H}_{h,\tau=0} = \lim_{\tau \rightarrow 0} \hat{H}_h^{n+1/2}(\tau)$$

are the solutions of Equation (12):

$$j\omega \hat{E}_{h,\tau=0} = \frac{1}{\varepsilon} \nabla_h \times \hat{H}_{h,\tau=0} - \frac{\sigma}{\varepsilon} \hat{E}_{h,\tau=0} + S_E, \quad (12a)$$

$$j\omega \hat{H}_{h,\tau=0} = -\frac{1}{\mu} \nabla_h \times \hat{E}_{h,\tau=0} - \frac{\sigma^*}{\varepsilon} \hat{H}_{h,\tau=0} + S_H. \quad (12b)$$

The stability condition to be satisfied for the above recursive scheme has been shown [12] to be

$$\frac{\tau}{h} \leq \sqrt{\frac{\varepsilon\mu}{8}}. \quad (13a)$$

However, we have recently shown that we can relax the above condition to read

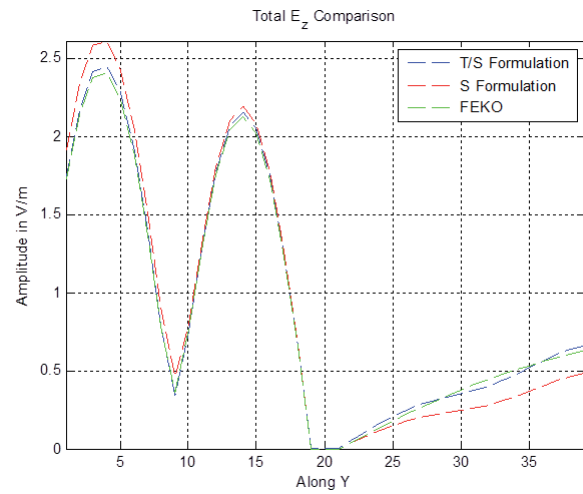


Figure 4b. A comparison of the amplitudes of the total  $E_z$  using different methods.

$$\frac{\tau}{h} \leq \sqrt{\frac{\varepsilon\mu}{3}}. \quad (13b)$$

Before closing this section, we mention that the Recursive Update in Frequency Domain can be formulated to work with either the scattered or total field formulations, providing it more flexibility than is available in the time-domain methods. It can also use either the Mur [14] or the PML boundary condition [15] for mesh truncation, depending on the accuracy desired.

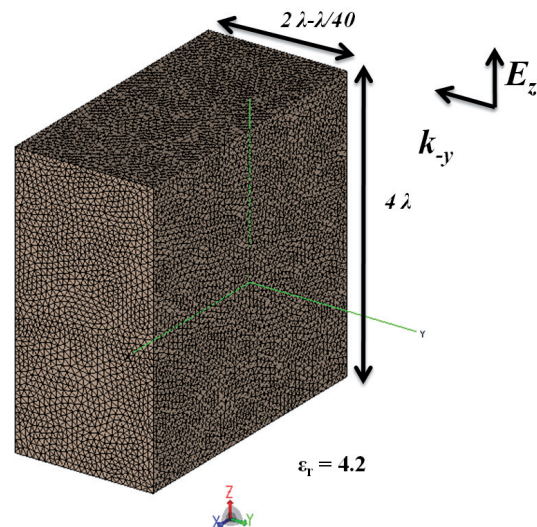


Figure 5. A dielectric cuboid.

	RUFD	FEKO
Simulation time [s]	19.63	20.5

Table 1. The Recursive Update in Frequency Domain simulation time compared with the commercial EM solver; FEKO.

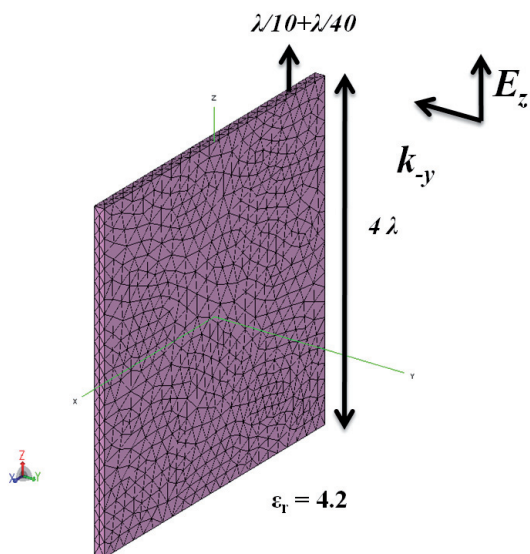


Figure 6a. The simulated dielectric slab.

### 3.3. Numerical Results

#### 3.3.1 PEC Scattering Problem

For the first example, we considered a PEC plate as shown in Figure 4a. Since the object was PEC, we had the flexibility in Recursive Update in Frequency Domain of using either the total or the scattered field formulation. The problem was solved by using both of these approaches, and the results are compared with FEKO in Figure 4b.

Even though the Recursive Update in Frequency Domain algorithm and the commercial MoM code took almost the same time for this PEC object, the proposed Recursive Update in Frequency Domain algorithm, which

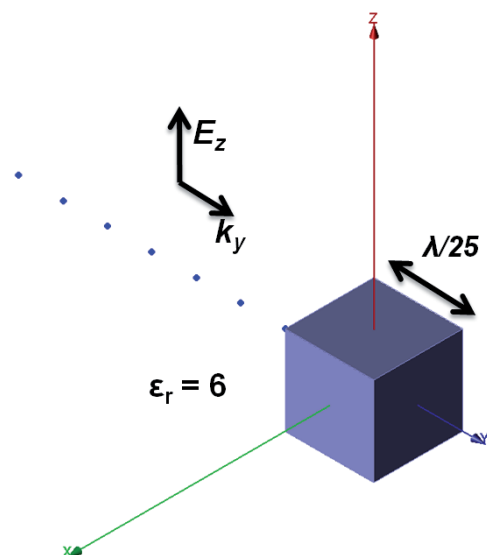


Figure 7a. The simulated dielectric cube.

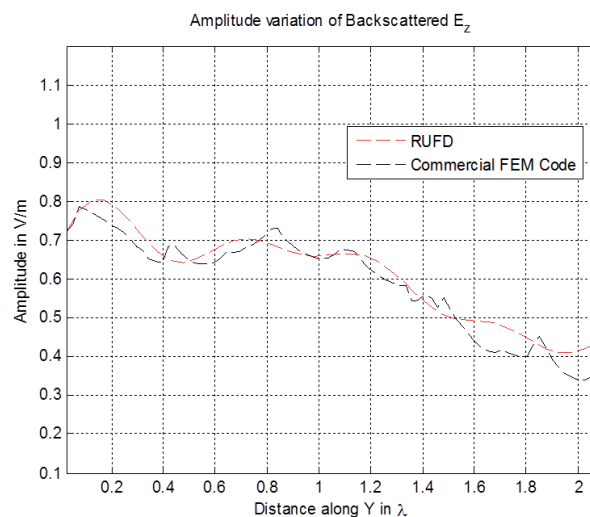


Figure 6b. A comparison of the amplitudes of the backscattered  $E_z$  using Recursive Update in Frequency Domain (RUF) and FEKO.

is a finite method, can handle finite conductivities and inhomogeneous objects much more numerically efficiently and accurately than can the MoM code, which can become numerically unstable. As an example, we mention the case of a lossless dielectric cuboid shown in Figure 5. The commercial MoM code couldn't reach a convergent iterative solution, while the Recursive Update in Frequency Domain was able to relatively easily handle it.

Turning next to finite methods, the accuracy of the Recursive Update in Frequency Domain results was superior to the commercial Finite-Element Method (FEM), even for the lossless case. As an example, we considered the lossless dielectric slab shown in Figure 6a. The problem was solved by using Recursive Update in Frequency Domain, and the results are compared with a commercial FEM code in Figure 6b. We mention that the case of lossy thin

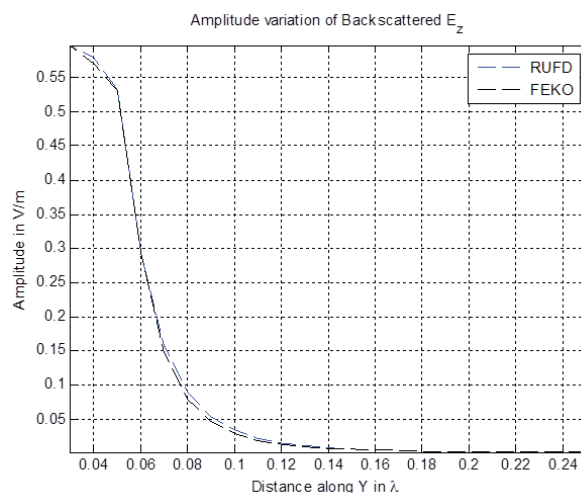


Figure 7b. A comparison of the amplitudes of the backscattered  $E_z$  using Recursive Update in Frequency Domain (RUF) and FEKO.



dielectrics is even more difficult to handle using existing finite methods, e.g., FEM.

### 3.3.2 Dielectric Scattering Problem

For the next example, we considered a dielectric cube, shown in Figure 7a. For this case, it was necessary for the Recursive Update in Frequency Domain to use the total-field formulation, since no convenient boundary condition is available for dielectric problems. The problem was solved in this manner, and the results are compared with *FEKO* in Figure 7b.

### 3.3.3 Scattering Problem Comprising a Combination of PEC and Dielectric

Numerical results for the fields scattered by a dielectric ( $\epsilon_r = 6$ ) layered conducting plate,  $\lambda_0$  on a side, under normal plane-wave illumination, are presented in Figures 8 and 9. The magnitude and phase variations of the scattered dominant component were computed varying  $y$  (expressed in cells) from 1 to 51. Perfectly matched layer (PML) boundary conditions were implemented in the code to terminate the computational domain.

The results were compared against existing commercial codes implementing different numerical techniques: *FEKO* (MoM), *HFSS* (FEM), and *CST* (Finite Integration Technique – FIT). The discretization for all EM solvers was kept around  $\lambda_0/20$ , while all the simulations were carried out using 4 GB RAM and a 3.0 GHz Intel Core 2 Duo processor. The performance benchmarks in terms of memory requirements and running times are displayed in Table 2.

The Recursive Update in Frequency Domain algorithm results were seen to be faster and less memory-demanding when compared to several different commercial solvers, but without a compromise in the accuracy. Furthermore, the Recursive Update in Frequency Domain almost always yielded more stable and accurate results than the other solvers.

### 3.3.4 Dipole Antenna

For the last example, we considered a radiation-type problem, as opposed to the scattering problems we have

discussed thus far. We analyzed a dipole antenna, shown in Figure 10a. Since this was a radiation-type problem, it was natural to use the total-field formulation in the context of the Recursive Update in Frequency Domain. The problem was solved in this manner, and the results are compared with *FEKO* in Figure 10b. The Recursive Update in Frequency Domain results were found to be the more accurate of the two.

## 3.4 Observations

As alluded to in Section 3.2, the Recursive Update in Frequency Domain algorithm is highly parallelizable. This is because unlike the FEM, it utilizes the difference form of Maxwell’s equations. Since the Recursive Update in Frequency Domain uses Yee’s cell, its meshing requirements are also relatively simple. Moreover, since the Recursive Update in Frequency Domain solves Maxwell’s equations in a recursive manner, without using either iteration or inversion, the problems of dealing with ill-conditioned matrices or constructing robust pre-conditioners are totally avoided. As a frequency-domain solver, it can also handle dispersive media, including plasmonics, relatively easily. To further enhance its performance, we can hybridize it with the Dipole Moment Approach, as shown in the next section. We can also use multi-grid methods or frequency-interpolation schemes to generate the initial values of the fields in the entire computational domain, enabling us to speed up the convergence.

## 4. The Hybrid DM/RUFD Technique for Multi-Scale Problems

Direct solution of multi-scale problems by means of conventional computational electromagnetics methods – be they FEM, FDTD, or MoM – is highly challenging, even with the availability of modern supercomputers. This is because of the large number of degrees of freedom introduced when attempting to accurately describe objects with fine features, sharing the computational domain with objects that are large compared to the operating wavelength.

Dealing with multi-scale objects often forces us to compromise the accuracy (relaxing the numerical discretization process when attempting to capture the small-scale features) in order to cope with the limited available resources in terms of CPU memory and time. In this section, we introduce a scheme that combines the Recursive Update

	<b>RUFD</b>	<b>HFSS</b>	<b>FEKO</b>	<b>CST</b>
Memory requirements (peak) [MB]	301	447.4	860.5	ph: 449.51 vir: 722.84
Simulation time [s]	79.2	132	377.49	215

Table 2. The Recursive Update in Frequency Domain simulation time and memory requirements compared with commercial EM solvers *HFSS*, *FEKO*, and *CST*.

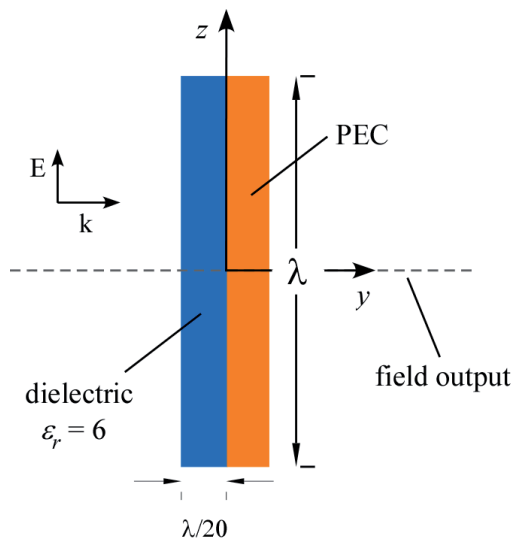


Figure 8a. The problem geometry.

in Frequency Domain and the Dipole Moment methods to solve multi-scale problems in a numerically efficient manner [16]. Our objective is to handle objects with fine features with the Dipole Moment approach, and not directly with the Recursive Update in Frequency Domain, which would require us to use a fine mesh (see Figure 11), at the cost of increased computational burden. The hybrid Dipole Moment/Recursive Update in Frequency Domain (DM/RUFD) method for addressing this type of problem was described in detail in [17]; we only highlight the main steps here and present a few illustrative examples.

The main advantage of the proposed hybrid method is that it does not require a local mesh refinement for objects with fine features (Figure 12). In fact, the region surrounding the small/thin structure is extracted from the

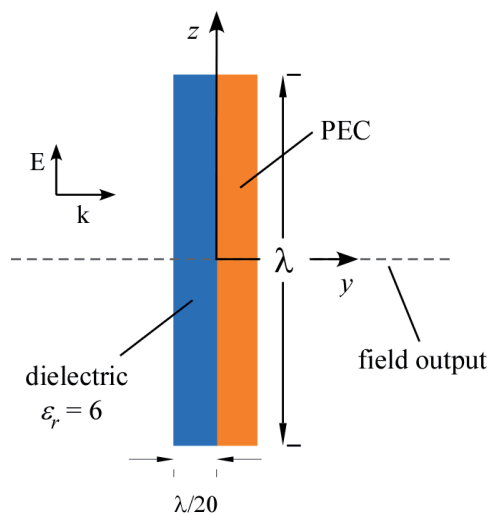


Figure 9a. The problem geometry.

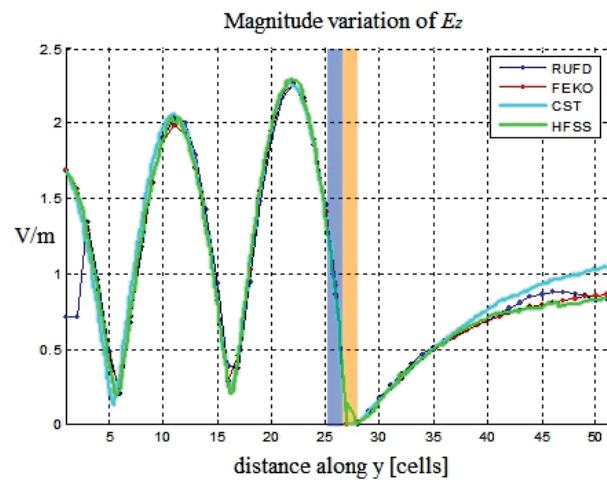


Figure 8b. The magnitude variation of the scattered  $E_z$  computed for varying  $y$  along all the computational domain at  $x = y = 0$ . Recursive Update in Frequency Domain results compared with FEKO, HFSS, and CST

original domain, and two different numerical techniques are used for dealing with the two problems. The coupling of the object with the remaining part of the computational domain is achieved by using the fields radiated by the previously extracted region. As a result, the presented method does not place a heavy burden on the CPU time and memory, as do the conventional approaches when dealing with multi-scale problems. The Dipole Moment/Recursive Update in Frequency Domain method introduced can be implemented either in an iterative or in a self-consistent manner.

The proposed method is especially useful for the modeling of wire antennas located in the vicinity of inhomogeneous structures, as well as for simulating interconnection structures in integrated circuits, which typically have fine features.

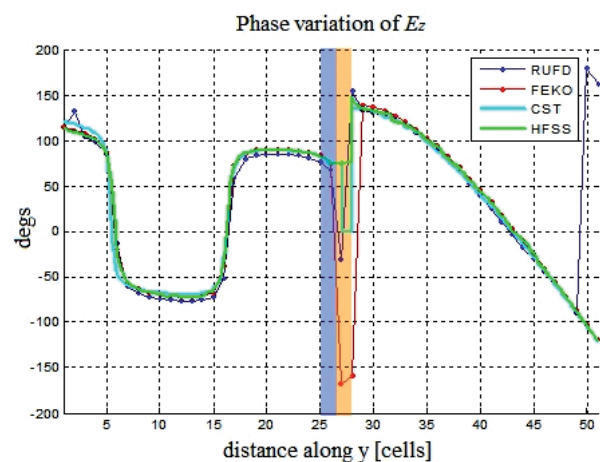


Figure 9b. The phase variation of the scattered  $E_z$  computed for varying  $y$  along all the computational domain (from cell 1 to cell 51) at  $x = y = 0$ . Recursive Update in Frequency Domain and FEKO, HFSS, and CST results were compared.

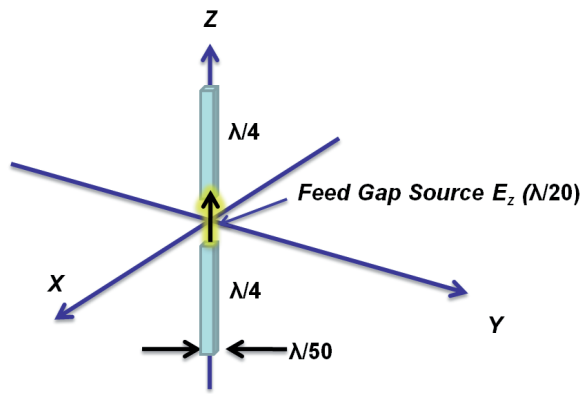


Figure 10a. The simulated dipole antenna

#### 4.1. Dipole Moment/Recursive Update in Frequency Domain Hybrid Scheme: Iterative Approach

Both the hybrid and self-consistent implementations (the latter to be described in the following section) begin by extracting from the Recursive Update in Frequency Domain technique's domain,  $\Sigma$ , a region  $\partial\Sigma$  surrounding the small object (for a two-dimensional representation of the hybrid problem, see Figure 13).

Let us assume that two objects, a large PEC plate and a PEC wire that is small compared to the operating wavelength, are located in the Recursive Update in Frequency Domain computational domain, which is illuminated by a plane-wave source. The hybrid-iteration algorithm begins by solving the large problem in the absence of the thin structure.

The fields scattered by the small structure are next derived by using a source excitation comprising of a combination of the original plane wave and the fields scattered by the large structure. The small object, which may be PEC, dielectric, or a combination thereof, is treated by using the Dipole Moment approach described in Section 2.3, and a matrix system is constructed. The right-

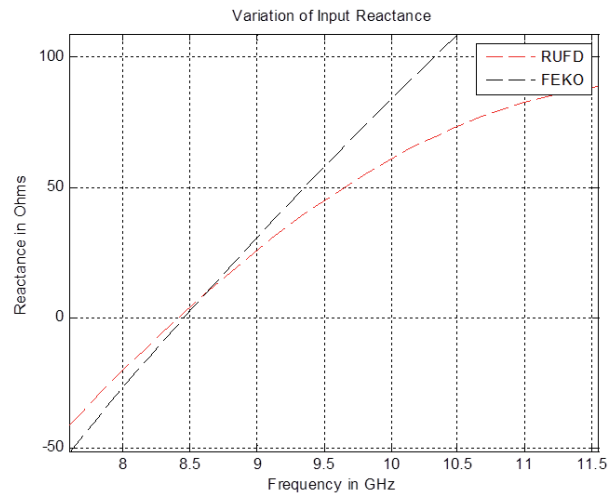


Figure 10b. The frequency variation of the input reactance using the Recursive Update in Frequency Domain (RUF) and FEKO.

hand side of this equation is the field incident upon each of the constitutive dipole moments. It is represented by the superposition of both the original plane-wave source and the field scattered by the larger structure. These fields are evaluated at the boundary of the extracted region,  $\partial\Sigma$  and are interpolated to obtain the  $N$  incident fields at each sphere's location (see Figure 13a for the example of a wire going across four Recursive Update in Frequency Domain cells).

Once the matrix system for the weight coefficients of the dipole moments has been solved, we can derive the scattered field (first iteration) inside the domain by superposing all dipole-moment contributions and the previously derived fields scattered by the large object. The iteration is subsequently continued by following the same steps as above, except for the fact that at the  $k$ th step, the incident plane wave is replaced by the scattered field derived in the  $(k-1)$ th iteration. The process is terminated when numerical convergence has been achieved, i.e., when the difference between the results obtained at the  $k$ th and  $(k-1)$ th iteration steps is below a chosen threshold. Figure 14 summarizes the basic steps for the scheme in a flowchart.

#### 4.2. Dipole Moment/Recursive

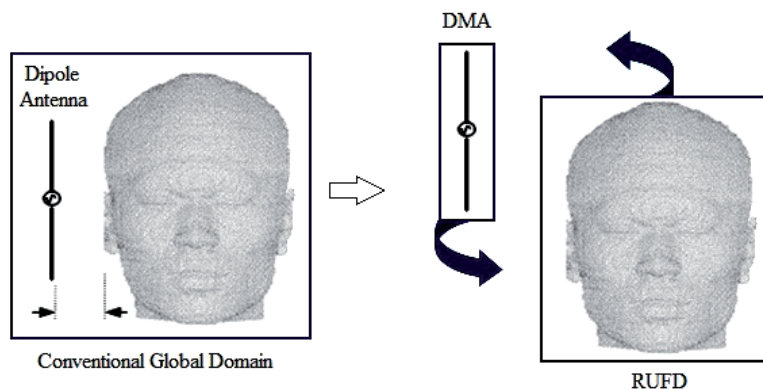


Figure 11. (a) The conventional solution of a multi-scale problem comprising a small object that shares the domain with a large object, and (b) the Dipole Moment/Recursive Update in Frequency Domain concept.

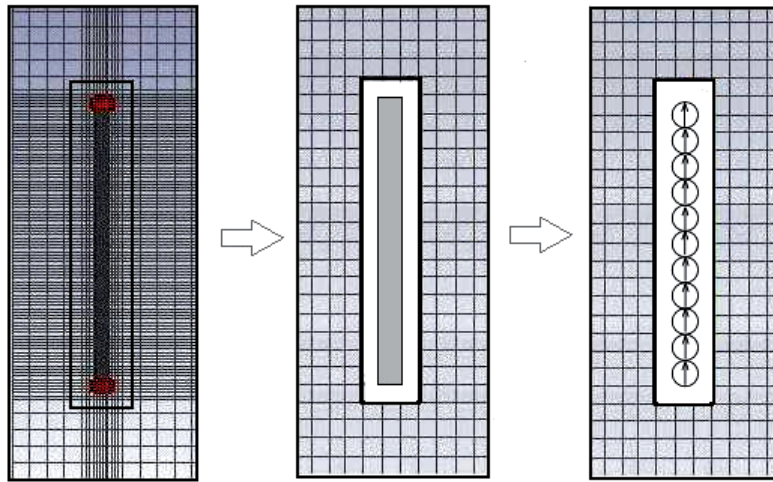


Figure 12. (a) A conventional volume discretization when dealing with a small structure, (b) the extraction of the region surrounding the small object in the Dipole Moment/Recursive Update in Frequency Domain, and (c) The discretization of the object in the extracted region with Dipole Moment.

### Update in Frequency Domain Hybrid Scheme: Self-Consistent Approach

The self-consistent implementation also begins by extracting a region  $\partial\Sigma$  surrounding the small object (as shown in Figure 13a) from the Recursive Update in Frequency Domain technique's domain. However, this time, the entire problem is solved in a single step by directly inverting a composite matrix equation, which is constructed as follows. First, the impedance matrix,  $\mathbf{Z}$ , for the small problem is set up independently of the rest by using the Dipole-Moment approach. The right-hand-side vector for plane-wave incidence is computed and stored (we will refer to it as to  $rhs_1$ ). Next, the large problem is solved with the Recursive Update in Frequency Domain in the absence of the thin structure for the original plane-wave source. The scattered fields are computed and interpolated at the small object's location, getting a new excitation vector for the Dipole Moment system ( $rhs_2$ ).

We compute the field radiated by the current

distribution on the small object at the location of the large object. We solve it by imposing the boundary condition on its surface, using the fields produced by the small object as the incident field on the large object.

The fields scattered by the large object are computed and interpolated at the small object's region, getting  $rhs_3$ . The matrix equation for the small object is set as follows:

$$\mathbf{Z}\underline{x} = -\underline{rhs}_1 - \underline{rhs}_2 - \underline{rhs}_3, \quad (14)$$

which indicates that the amplitude of the third term on the right-hand side is still to be determined. We obtain the above by using

$$(\mathbf{Z} + \underline{rhs}_3)\underline{x} = -(\underline{rhs}_1 + \underline{rhs}_2), \quad (15)$$

and solve the matrix equation for the weights of the

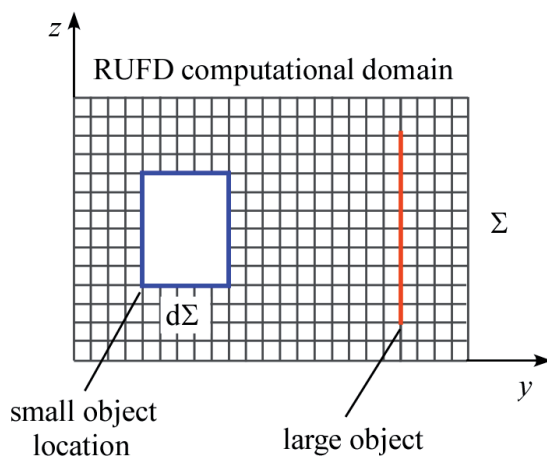


Figure 13a. A two-dimensional representation of a conventional hybrid problem in the Recursive Update in Frequency Domain technique's domain.

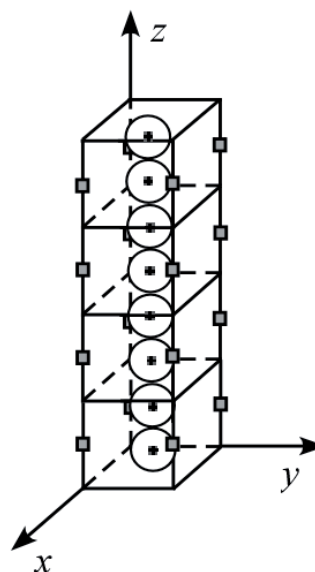


Figure 13b. A small wire, described by equivalent Dipole Moments, which extends through four Recursive Update in Frequency Domain cells.

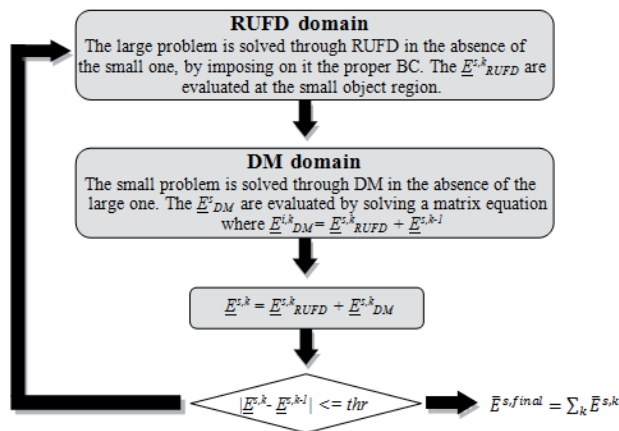


Figure 14. The flowchart for the iterative hybrid Dipole Moment/Recursive Update in Frequency Domain scheme.

currents  $\underline{x}$ . The final scattered fields are calculated as a weighted superposition of the three contributions as

$$E^{s,f} = E^{s,1} + E^{s,2} + \chi E^{s,3} \quad (16)$$

A flowchart for the steps followed in the self-consistent scheme is displayed in Figure 15. Since the procedure is non-iterative, its running time is more favorable than that of the iterative approach.

While the above scheme works well when only PEC structures are involved as large objects, we need to modify it slightly when the large object is a combination of PEC and dielectric materials. For the details of the modified procedure, the reader is referred to [14].

### 4.3 Numerical results

In this section, some numerical results are presented for the two different hybrid techniques. The numerical efficiency over existing methods, both in terms of running

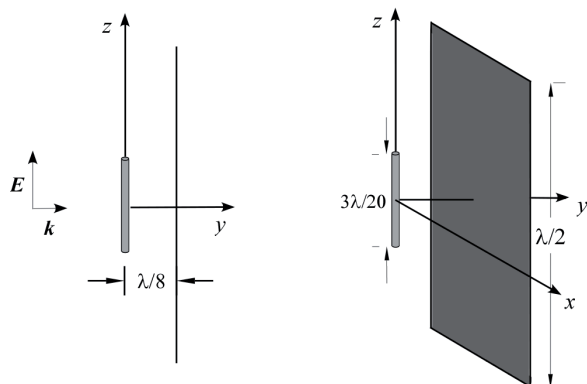


Figure 16a. The problem geometry.

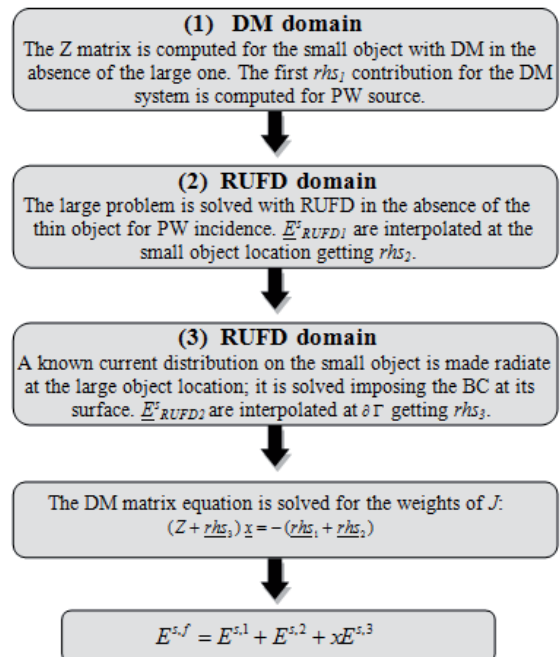


Figure 15. The flowchart for the self-consistent Dipole Moment/Recursive Update in Frequency Domain hybrid scheme.

times and memory requirements, is demonstrated via several examples.

#### 4.3.1 PEC Sheet in the Presence of a $3\lambda/20$ Conducting Wire

Numerical results for the fields scattered by a conducting plate,  $\lambda_0/2$  on a side, under normal plane-wave illumination in the presence of a PEC wire, the length of which is  $3\lambda/20$ , are presented in Figures 16 and 17. The

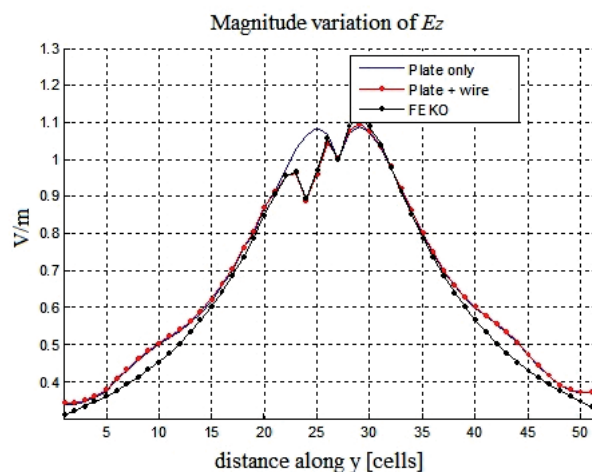


Figure 16b. The magnitude variations of scattered  $E_z$  computed for varying  $y$  along all the computational domain (from cell 1 to cell 51) at  $x = y = 0$ . Recursive Update in Frequency Domain and FEKO results were compared.

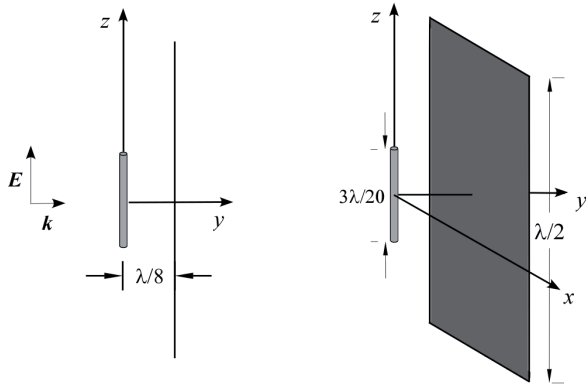


Figure 17a. The problem geometry.

magnitude and phase variations of the scattered dominant component were computed for varying  $y$  (expressed in cells) from 1 to 51. The PEC sheet was located at cell  $y = 27$ , while the wire was located at a distance of  $0.125\lambda$  from the sheet, i.e., 2.5 cells away from the sheet along  $y$ . A plane-wave source was incident along  $y$ , with its  $E$ -field vector polarized along  $z$ . Absorbing boundary conditions (ABCs) were used to terminate the computational domain for this simulation. The results in the absence and in the presence of the wire were compared against commercial MoM software results. Good agreement with conventional MoM was achieved in this simulation.

### 4.3.2 PEC Sheet in the Presence of a $\lambda/2$ Conducting Wire

We next investigated the performance of the hybrid Dipole Moment/Recursive Update in Frequency Domain iterative and self-consistent approaches, both in terms of runtime and accuracy. This was done for the problem of scattering by a PEC sheet that was  $1\lambda$  on a side, and had a  $\lambda/2$  conducting wire located in close proximity to the sheet. An  $E_z$  polarized plane wave was normally incident on the structure. The relative distance between the sheet and the wire was the same as in the previous example (Figure 17a). The two hybrid schemes are compared in terms of accuracy against existing commercial codes implementing different numerical techniques – FEKO (MoM), HFSS (FEM), and CST (FIT) – in Figures 18 and 19. The efficiency of the two hybrid methods is compared in terms of running time and memory requirements in Table 3. The cell size was kept as  $\lambda_0/20$ , and the PML boundary conditions were implemented for simulating both hybrid Dipole Moment/Recursive Update in Frequency Domain cases. All the

	Hybrid DM/RUFD Self Consistent	Hybrid DM/RUFD Iterative
Memory requirements (peak) [MB]	483	481
Simulation time [s]	172.3	601

Table 3. The hybrid Dipole Moment/Recursive Update in Frequency Domain iterative and self-consistent implementations compared in terms of simulation time and memory requirements (the cell size was  $\lambda/20$ , and PML boundary conditions were used).

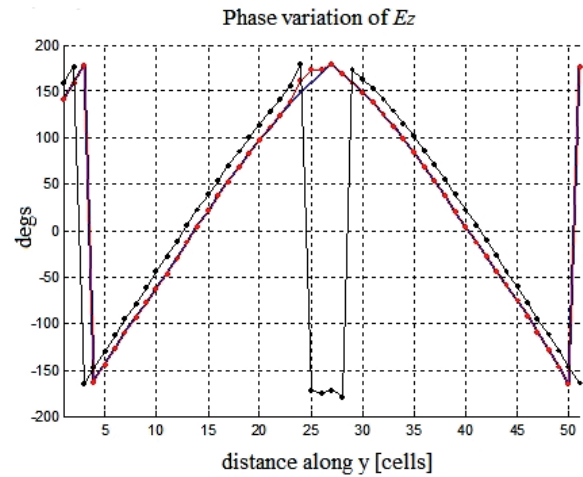


Figure 17b. The phase variations of scattered  $E_z$  computed for varying  $y$  along all the computational domain (from cell 1 to cell 51) at  $x = y = 0$ . Recursive Update in Frequency Domain and FEKO results were compared.

simulations were carried out on a personal computer with 4 GB RAM and a 3.0 GHz Intel Core 2 Duo processor.

We noted from Figures 18 and 19 that the iterative Dipole Moment/Recursive Update in Frequency Domain hybrid approach provided better performance in terms of accuracy. It was apparent from Table 3 that the self-consistent approach was more efficient. The memory requirements were comparable for the two options.

### 4.3.3 Dielectric-Coated PEC Sheet in the Presence of a $\lambda/2$ PEC Wire

In the following test example, we considered a PEC plate that was coated with  $\lambda/10$ -thick dielectric ( $\epsilon_r = 6$ ), and which shared the computational domain with a  $\lambda/2$ -long conducting wire. These objects were illuminated by a plane wave that propagated along the  $y$  axis, with its  $E$ -field vector polarized along  $z$  (Figure 20). The total field distribution computed by the present approach is compared against commercial codes implementing the MoM (FEKO), the FEM (HFSS), and the FIT (CST) in Figure 21. Note that satisfactory agreement was achieved with HFSS and CST, both in amplitude and in phase (see Figure 21), while the commercial MoM results were not as accurate for this example.

The performance in terms of running time and memory requirements are displayed in Table 4. We also noted from

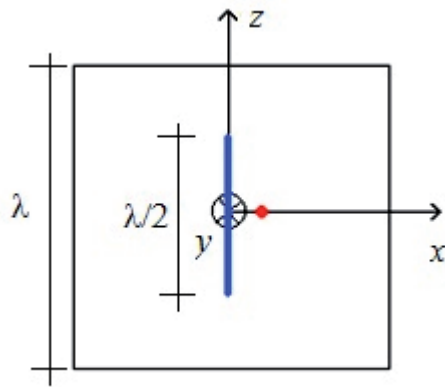


Figure 18a. The problem geometry.

this table that the Hybrid Dipole Moment/Recursive Update in Frequency Domain code performed better than either CST or HFSS, both in terms of memory and running time. Although the simulation time for the Recursive Update in Frequency Domain was comparable to that of the MoM code, the latter did not generate accurate results for this case, as noted earlier. We believe that the inaccuracies stemmed from the difficulty with the MoM technique when dealing with thin, inhomogeneous structures. As we also saw from Table 4, the finite methods paid a toll in terms of increased memory and running times, owing to the use of fine meshes when dealing with multi-scale problems.

#### 4.4. Enhancements of the Dipole Moment and Recursive Update in Frequency Domain Techniques

I

- Applies novel techniques to deal with problems at low frequencies.
- Enhances the convergence of the recursive update scheme by applying signal-processing techniques to the time signature.
- Uses the above signal-processing techniques and derives

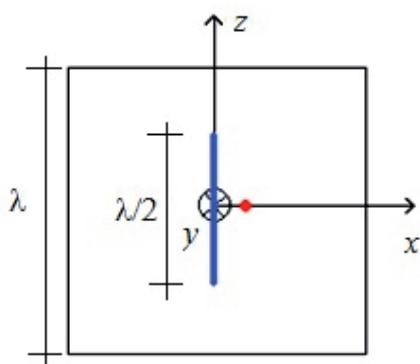


Figure 19a. The problem geometry.

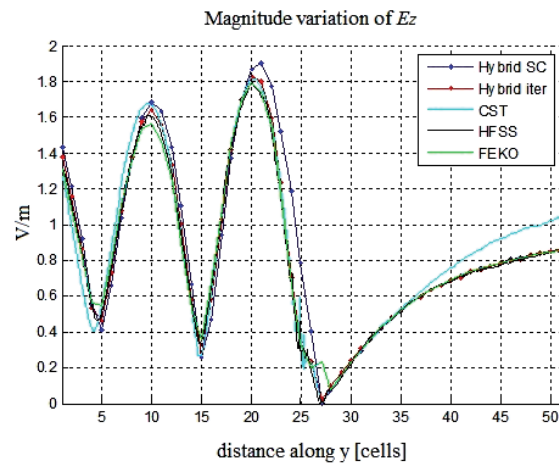


Figure 18b. The magnitude variation of scattered  $E_z$  computed for varying  $y$  along all the computational domain (from cell 1 to cell 51).

the solution for multiple frequencies in a single run, enhancing the computational efficiency of the original Recursive Update in Frequency Domain algorithm quite significantly in the process.

- Handles dispersive media, as well as those with negative  $\epsilon$  and  $\mu$  as long as the material can be represented by using either Debye or Drude models.

To illustrate the numerical efficiency of the vCFDTD relative to the Recursive Update in Frequency Domain, we considered the waveguide filter shown in Figure 22, which is a high- $Q$  structure. Table 5 compares the number of iterations required to solve the waveguide filter shown in Figure 22. The time advantage of vCFDTD over Recursive Update in Frequency Domain was evident.

The results of these embellishments to the Dipole Moment and Recursive Update in Frequency Domain algorithms will be reported in future publications.

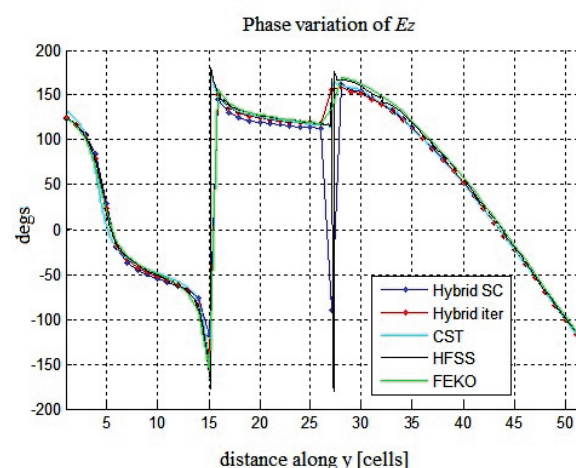


Figure 19b. The phase variation of scattered  $E_z$ : the results of the hybrid Dipole Moment/Recursive Update in Frequency Domain iterative and self-consistent were compared with commercial MoM, FEM, and FIT solvers.

	Hybrid DM/ RUFDF Self Con- sistent	FEKO	CST	HFSS
Memory require- ments (peak) [MB]	348	690.6	ph: 1590 vir: 1910	1680
Simulation time [s]	260	284.12	1565	1861

Table 4. The performance of the hybrid and self-consistent Dipole Moment/ Recursive Update in Frequency Domain implementation, compared with FEKO, CST, and HFSS in terms of the simulation time and memory requirements (the discretization was  $\sim \lambda/20$ ).

## 5. Conclusion

In this work, we have introduced some novel concepts in computational electromagnetics (CEM) that deviate from the conventional MoM, both in terms of their formulation as well as their solution of radiation and scattering problems. We have shown how MoM-type problems can be formulated by using Dipole Moments, without the use of Green's functions. We have argued that the Dipole Moment formulation offers us a way to formulate the computational electromagnetics problems involving PEC as well as dielectric objects in a uniform manner. The Dipole Moment formulation also mitigates the so-called low-frequency problem, and is well suited for handling multi-scale problems.

The Recursive Update in Frequency Domain approach, which has the versatility of the FDTD method, may be viewed as the frequency-domain version of the FDTD algorithm. However, unlike the FEM, it does not rely on the solution of a matrix equation, either directly or iteratively, but generates the solution via a recursive procedure, instead. We have shown how the Dipole Moment and Recursive

	RUFDF	vCFDTD
Required Number of Iterations	37500 >	6000

Table 5. The performance of vCFDTD in terms of the required number of iterations compared with the Recursive Update in Frequency Domain.

Update in Frequency Domain algorithms may be combined to accurately and efficiently solve multi-scale problems. The performance of the resulting hybrid scheme has been found to be superior to those of some of the well-known and widely used computational electromagnetics codes, both in terms of accuracy and computational efficiency. Enhancements to the basic Dipole Moment and Recursive Update in Frequency Domain algorithms – such as for instance the vCFDTD and its hybridization with Dipole Moment – which would further enhance their performances are currently being actively investigated. The preliminary outlook appears to be quite promising, indeed.

## 6. References

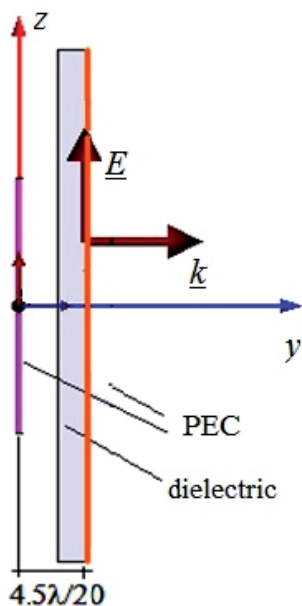


Figure 20a. A two-dimensional cut of the problem geometry.

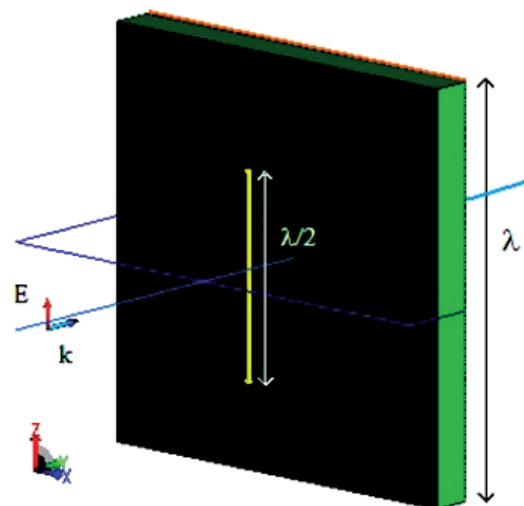


Figure 20b. A three-dimensional representation of the problem geometry.



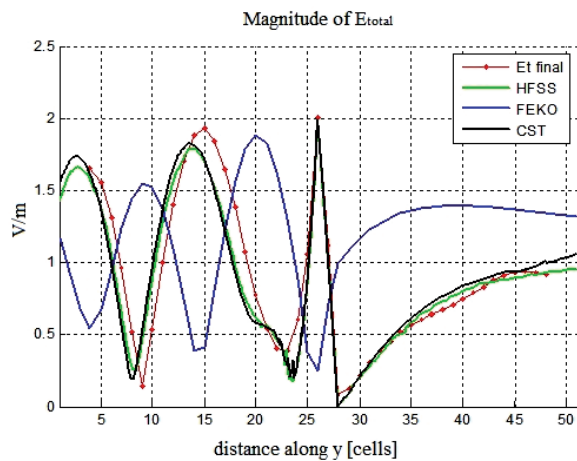


Figure 21a. The magnitude variations of the final total fields along the y axis. The results computed through the modified self-consistent hybrid scheme were compared with FEKO, HFSS, and CST.

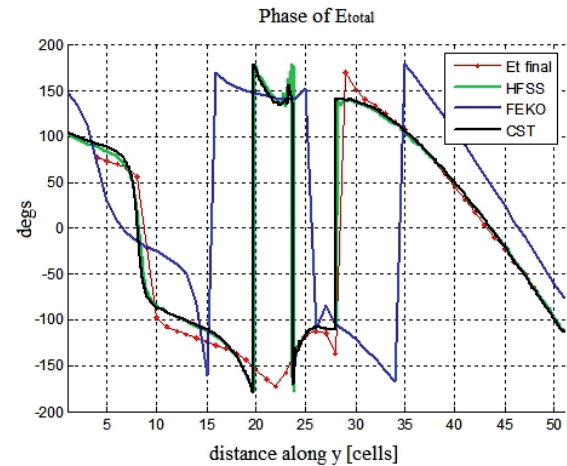


Figure 21b. The phase variations of the final total fields along the y axis. The results computed through the modified self-consistent hybrid scheme were compared with FEKO, HFSS, and CST.

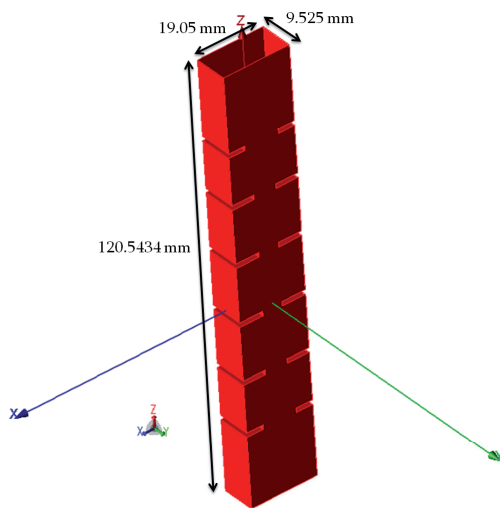


Figure 22. A waveguide filter.

1. B. T. Draine and P. J. Flatau, "Discrete-Dipole Approximation for Scattering Calculations," *J. Opt. Soc. Am. A*, **11**, April 1994, pp. 1491-1499.
2. R. F. Harrington, *Field Computation by Moment Methods*, New York, The Macmillan Company, 1968.
3. R. Mittra, *Computer Techniques for Electromagnetics*, New York, Hemisphere Publishing Corporation, 1987.
4. A. F. Peterson, S. L. Ray, and R. Mittra, *Computational Methods for Electromagnetics*, New Jersey, IEEE Press, 1997.
5. R. Mittra, K. Panayappan, C. Pelletti and A. Monorchio, "A Universal Dipole-Moment-Based Approach for Formulating MoM-Type Problems without the Use of Green's Functions," Proceedings of the European Conference on Antennas and Propagation 2010, Barcelona, April 2010.
6. R. Harrington, *Time-Harmonic Electromagnetic Fields*, Piscataway, NJ, IEEE Press, 2001.

7. J. Bringuier, *Multi-scale Techniques in Computational Electromagnetics*, PhD dissertation, Pennsylvania State University, 2010.
8. E. C. Jordan and K. G. Balmain, *Electromagnetic Waves and Radiating Systems*, Upper Saddle River, NJ, Prentice Hall, 2001.
9. C. Pelletti, R. Mittra, K. Panayappan and A. Monorchio, "A Universal and Numerically Efficient Method of Moments Formulation Covering a Wide Frequency Band," IEEE International Symposium on Antennas and Propagation and USNC/URSI National Radio Science Meeting, Spokane, Washington, July 3-8, 2011.
10. E. Lucente, A. Monorchio, and R. Mittra, "An Iteration-Free MoM Approach Based on Excitation Independent Characteristic Basis Functions for Solving Large Multiscale Electromagnetic Scattering Problems," *IEEE Transactions on Antennas and Propagation*, **AP-56**, April 2008, pp. 999-1007.
11. S. J. Kwon and R. Mittra, "Impedance Matrix Generation by Using Fast Matrix Generation (FMG) Technique," *Microwave and Optical Technology Letters*, **51**, January 2009, pp. 204-213.
12. C. Pflaum and Z. Rahimi, "An Iterative Solver for the Finite-Difference Frequency-Domain (FDFD) Method for Simulation Of Materials With Negative Permittivity," *Numer. Linear Algebra Appl.*, **18**, 4, August 2011, pp. 653-670.
13. K. S. Yee, "Numerical Solution of Initial Boundary Value Problems Involving Maxwell's Equations in Isotropic Media," *IEEE Transactions on Antennas and Propagation*, **AP-14**, 3, May 1966, pp. 302-307.
14. G. Mur, "Absorbing Boundary Conditions for the Finite-Difference Approximation of the Time-Domain Electromagnetic Field Equations," *IEEE Transactions on Electromagnetic Compatibility*, **23**, 3, 1981, pp. 377-382.
15. J. P. Berenger, "Three-Dimensional Perfectly Matched Layer for the Absorption of Electromagnetic Waves," *J. Comp. Phys.*, **127**, 1996, pp. 363-379.
16. C. Pelletti, K. Panayappan, R. Mittra and A. Monorchio, "On the Hybridization of RUFDA Algorithm with the DM Approach for Solving Multiscale Problems," Proceedings of the 20th

International Symposium on EM Theory, Berlin, Germany,  
August 2010.

17.C. Pelletti, *Numerically Efficient Techniques for Electromagnetic Scattering Calculations in the Frequency Domain*, PhD dissertation, University of Pisa, 2011.